Numerical Analysis of the Power Saving in 3GPP LTE Advanced Wireless Networks

Sunggeun Jin, *Member, IEEE*, and Daji Qiao, *Member, IEEE*

***Abstract*—We analyze the power-saving operation in Third–Generation Partnership Project (3GPP) Long-Term Evolution Advanced (LTE Advanced) wireless networks. Typically, it is an exhausting and complicated job to numerically analyze the performance of power-saving operations since it is necessary to carefully consider every possible probability, make probability-generating functions, and differentiate these functions. Instead, we develop a totally new approach toward simple but accurate derivations. For this purpose, we divide the time period for the steady-state power-saving operation into several independent parts. Then, we analyze the power-saving operation in each part and thereafter combine the results into an aggregate result. The new approach enables us to avoid sophisticated steps while we reach an accurate analytical model. The equations are validated through comparison with simulation results.**

***Index Terms*—Discontinuous reception (DRX), power saving, sleep mode.**

I. Introduction

MOST of today's wireless networks such as IEEE 802.11 wireless local area networks, IEEE 802.16 wireless metropolitan area networks, and Third-Generation Partnership Project (3GPP) Long-Term Evolution Advanced (LTE Advanced) wireless networks provide power-saving operations since lifetime extension of battery-powered mobile devices is one of the most important features for user convenience [2]–[4], [6], [15], [16]. Accordingly, LTE Advanced wireless networks support the power-saving operation called Discontinuous Reception (DRX) operation, whereas one or more user equipment (UE) are serviced with lightly loaded and/or periodic traffic [5]. In the DRX operation, the UE periodically wakes up to monitor new packet arrivals by receiving an indication message conveyed via a control channel, i.e., the physical downlink control channel. If the UE receives a positive indication message indicating that newly arrived packets are buffered and ready for transmissions at the radio network controller (RNC), it stays awake to receive the buffered packets. Otherwise, it immediately goes back to sleeping to prevent redundant power consumption. Typically, the performance of the power-saving operation can be evaluated with two metrics, i.e., the power-saving factor and the average packet transmission delay. The power-saving factor is defined by a ratio between sleeping time and overall operation time [26].

In the 3GPP LTE Advanced standard, many operational states are defined to control UE's operation [5]. However, in viewpoint of power consumption, we can characterize the DRX operation by two operational states, i.e., active and sleeping states, respectively. The active-state UE keeps awake to receive packets with an activated transceiver. In contrast, the sleeping-state UE inactivates its transceiver and hence needs to periodically wake up to receive an indication message. Prior to the beginning of sleeping state, the active-state UE initiates an *inactivity timer* to monitor new packet arrivals. If one or more new packets arrive before the timer's expiration, the UE staying in active state restarts the timer after completing the receptions of newly arrived packets. Otherwise, the operational state transits to sleeping state.

Over the past few years, much effort have been made to analyze the performance of the power-saving operation [7]–[9], [11], [12], [14], [18], [20], [21], [24]–[30]. Yang and Lin [26] first provided an analytical model for the DRX operation in the Universal Mobile Telecommunications System [1], which is the former technology of the 3GPP LTE Advanced, assuming that packet arrival intervals and transmission times follow exponential and general distributions, respectively. Thereafter, the authors of [24], [25], [27], [30] extended the model for their purposes. However, their equation derivations are complicated, so that it is not easy to extend their work for further studies. We summarize their derivation steps since they follow a typical approach toward the performance analysis of the power-saving operation as follows:

In [24]–[27], and [30], the probabilities for all cases as to how many packets arrive depending on UE's power-saving operation while a packet is being served were first derived. From the probabilities, they utilize Z-transform leading to a probability generating function. Then, they differentiate the probability generating function to obtain average packet transmission delay. After that, they convert the Z-transform equations into Laplace transform equations. They continue to differentiate the Laplace transform equations to obtain the time durations for the active and sleeping states. Finally, they obtain the power-saving factor by dividing the sleeping state time duration by the overall operation time, which is equal to the active state time duration plus the sleeping state time duration.

In contrast, we present an accurate analytical model with a simple approach to the performance analysis of the

Manuscript received April 6, 2011; revised September 11, 2011 and December 5, 2011; accepted January 26, 2012. Date of publication Febraury 13, 2012; date of current version May 9, 2012. This work was supported in part by the Korea Communications Commission under the R&D program supervised by the Korea Communications Agency under Grant KCA-2011-09913-04006, by the Information Infrastructure Institute of Iowa State University, and by the U.S. National Science Foundation under Grant CNS 0831874. The review of this paper was coordinated by Dr. C.-C. Chong.

S. Jin is with ETRI, Daejeon 305-700, Korea (e-mail: sgjin@etri.re.kr).

D. Qiao is with the Department of Electrical and Computer Engineering, Iowa State University, Ames, IA 50011 USA (e-mail: daji@iastate.edu).

Digital Object Identifier 10.1109/TVT.2012.2187690

power-saving operation in wireless access networks. Then, we apply the presented model to the 3GPP LTE Advanced power-saving operation. For this purpose, we follow totally different steps from the previous derivations in [13], [21], [24]–[27], [29], and [30]. We divide the DRX operation into several parts, and then, we combine the results obtained from each part into an aggregate result. For the analytical study, we have the same assumption as what Yang and Lin [26] made. In other words, packet arrival intervals and transmission times follow exponential and general distributions, respectively. We assume that the RNC allocates a single-transmission buffer for each UE, and the transmission buffer can accommodate an infinite number of packets.

In summary, we first consider power-saving operation in the steady state. The steady-state power-saving operation is divided into two stationary parts, i.e., the operation in active and sleeping states, respectively. As we will explain later, the proposed approach gives us an easy way to derive the expected time duration that the UE spends in each stationary part. Once we obtain the time durations in active and sleeping states, it is simple to have the power-saving factor. Then, we continue to use these time durations to derive the average packet transmission delay.

As explained earlier, when the UE performing the DRX operation is in sleeping state, the RNC buffers newly arrived packets without transmissions. Immediately after returning to active state, the UE begins to receive buffered packets. When RNC's transmission buffer becomes empty, the UE initiates an inactivity timer. As long as the inactivity timer is not expired, newly arrived packets are queued for immediate transmissions. To efficiently handle the packet transmission delay, we introduce two more states of immediate transmitting, and buffering and forwarding.

When the UE is in immediate-transmitting state, the packets suffers delay due to residual time. Residual time is defined by the time required to complete packet transmissions of all packets remaining in the transmission buffer, as well as ongoing packet transmission when a packet arrives at an arbitrary time. We find out that the delay due to the residual time is modeled by a M/G/1 queuing system. The *Pollaczek-Khinchine* $(P - K)$ *formula* presents packet transmission delay for a typical M/G/1 queuing system [23].

Meanwhile, let us consider a system having two operating time periods, depending on whether packet transmissions are allowed or not. In the first operating time period, packet transmissions are not allowed, and hence, arriving packets are buffered in the system. However, in the subsequent operating time period, the system forwards the buffered packets. Levy and Kleinrock [19] showed that a packet arrival during the time period in which packet transmissions are not allowed may suffer two types of independent delays until completing the transmission for the packet in the considered system. We rearrange their finding in terms of the DRX operation in 3GPP LTE Advanced networks. The first one is innate delay generated for the same reason as the delay incurred by the residual time in immediate-transmitting state. The other one is caused by RNC's buffering operation due to the time period during which packet transmissions are not allowed. Additionally, the authors proved that overall delay can be represented by the sum of both types of delays.

In buffering-and-forwarding state, the RNC does not transmit but buffers packets during sleeping state and thereafter transmits the buffered packets during active state. We realize that we can employ the feature found in [19] that two types of delays can be independently handled in the time period subsequent to the duration in which packet transmissions are not allowed. By using the feature, we derive the delay for the case when the UE is in buffering-and-forwarding state. Again, we apply the M/G/1 queuing model to the derivation of packet transmission delay when the RNC forwards buffered packets in buffering-and-forwarding state. In addition, we provide new derivations for the delays caused by RNC's buffering operation in detail. Then, we obtain an overall delay in buffering-and-forwarding state by considering the probabilities that both types of delays may occur in the state.

This paper is organized as follows: In Section II, we briefly explain 3GPP LTE Advanced power-saving operation. In Section III, we numerically analyze the performance of the 3GPP LTE Advanced power-saving operation in terms of the power-saving factor and average packet transmission delay according to the proposed derivation steps. In Section IV, we evaluate the performance and validate the correctness of the equations with simulation results. Section V concludes this paper.

II. Discontinuous Reception Operation in Third-Gerneration Partnership Project Long-Term Evolution Advanced Wireless Networks

Fig. 1 shows an exemplary operation for the case when a UE conducts the DRX operation to reduce unnecessary power consumption. A DRX cycle is a time duration that the UE periodically wakes up to monitor new packet arrivals. At the beginning of the DRX cycle, the UE temporarily stays awake to receive an indication message. When the UE receives a negative indication message, it goes back to sleeping. On the other hand, upon reception of a positive indication message, the UE stays awake to receive buffered packets. Indication message transmission time is very short and hence neglected in our analysis. In this figure, DRX cycles are denoted by rectangles, with letters "S" and "L" standing for short and long DRX cycles, respectively.

As shown in this figure, we define four operational states for proper analysis. Additionally, we define *activity period* by the time duration from time instant that the RNC begins to transmit packets under the condition that the RNC is not transmitting packets in either active or sleeping state to the time instant that RNC's buffer becomes empty due to the completion of packet transmissions. The *first activity period* is defined by the activity period, following DRX cycles. Meanwhile, the 3GPP LTE Advanced standard specifies that the *inactivity period* is the time duration when an inactivity timer is activated.

In active state, the UE receives packets during activity periods or waits for new packet arrivals within inactivity timer's timeout. For example, when RNC's buffer becomes empty after completing buffered packet transmissions, the UE activates an inactivity timer prior to the beginning of sleeping state. Unless

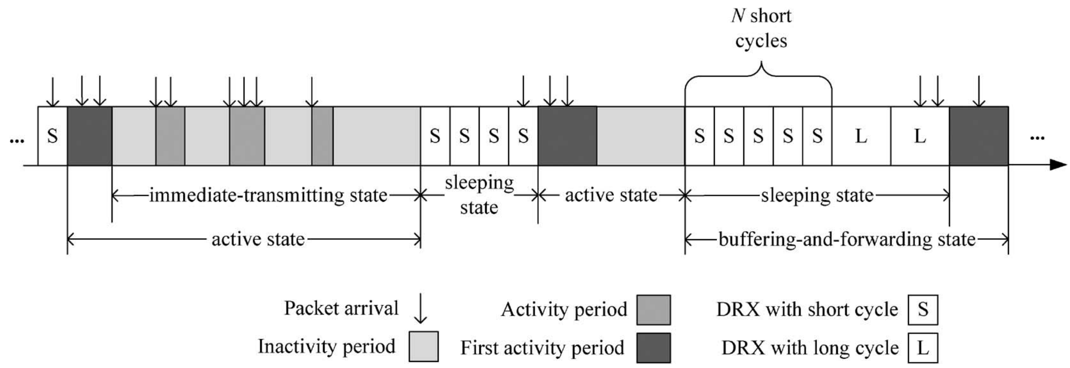

Fig. 1. Exemplary snapshot of the DRX operation in 3GPP LTE Advanced wireless networks.

there arrives a new packet within the timer expiration, the UE enters sleeping state. Otherwise, a new activity period begins for the UE to receive the newly arrived packets. The activity period can be extended as long as more packets arrive at the RNC during ongoing packet transmission times. Therefore, in active state, the activity period interleaved with the inactivity period repeats until the inactivity timer expires.

Sleeping state begins with the inactivity timer's expiration. In sleeping state, the UE monitors new packet arrivals at the RNC by periodically receiving indication messages every DRX cycle. DRX cycles follow back to back until new packet arrivals. If the UE detects new packet arrivals, the operational state transits to active state for the UE to receive those packets during the activity period. Optionally, a short DRX cycle can be employed for more frequent packet arrivals than a long DRX cycle. There may exist services with aperiodic silent period or occasional packet arrivals. In this case, a long DRX cycle may be useful. Long DRX cycles begin after the maximum number $(= N)$ of short DRX cycles has passed without new packet arrivals. N is a configurable value. Note that active and sleeping states are defined to derive the power-saving factor while buffering-and-forwarding and immediate-transmitting states are defined for packet transmission delay analysis. Immediate-transmitting state includes only extended awake time durations after the first activity period. Accordingly, buffering-and-forwarding state deals with the operations for sleeping state and the first activity period.

III. Analytical Model

We assume that packet arrival intervals follow an exponential distribution of which expectation is $1/\lambda$. Transmission times are distributed in a general manner. Random variable X represents the transmission time for a single packet, and its expectation is denoted by $E[X](= \tau)$. The traffic intensity ρ is defined by $\rho = \lambda\tau$.

Fig. 2 shows an example for active state operation. As shown in this figure, random variable $\hat{t}_I$ represents the time from the beginning instant of an inactivity timer to the stopping instant of the timer due to a new packet arrival. Random variable t_B is used to indicate the subsequent activity period after the inactivity timer stops. The first activity period begins with the transmissions for the buffered packets during the last DRX cycle prior to the first activity period. Specifically, the time for the first activity period is denoted by $\tilde{t}_B$. Random variables

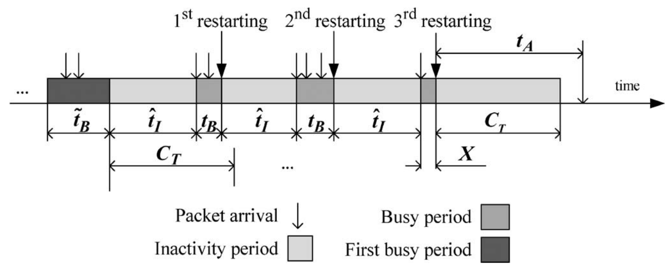

Fig. 2. Example for active state operation.

T_A and T_D indicate the overall times that the UE spends in active and sleeping states. Their expectations are denoted by $E[T_A]$ and $E[T_D]$, respectively. As specified in the 3GPP LTE Advanced wireless network standard [5], we adopt constant values C_T, C_S, and C_L for the inactivity timer, short DRX cycle, and long DRX cycle.

Since exponential distribution has memoryless property, it is true that $\Pr(t_I > X + C_T | t_I > X) = \Pr(t_I > C_T)$. For this reason, we can handle random variable $\hat{t}_I$ satisfying $t_I \leq C_T$ with a packet arrival interval distribution truncated by the timer timeout, i.e., truncated exponential distribution.

A. Power-Saving Factor

The power-saving factor was introduced to indicate the sleeping time ratio, compared with the overall operation time [26]. It is given by

$$E[T_D]/\left(E[T_A] + E[T_D]\right). \tag{1}$$

As seen in this equation, we need to derive $E[T_A]$ and $E[T_D]$. In the steady state, the UE's operation has independent and stationary operation time periods for active and sleeping states. It implies that we can independently obtain each time duration corresponding to active or sleeping state. The time duration for active state increases when a new packet arrives within inactivity timeout $(= C_T)$. Therefore, we can derive the new packet arrival probability by $\int_0^{C_T} \lambda e^{-\lambda t} dt = 1 - e^{-\lambda C_T}$. Similarly, sleeping state time extends until a packet arrives within a short or long DRX cycle. Accordingly, the probability for the sleeping state time extension can be derived by $\int_{C_S}^{\infty} \lambda e^{-\lambda t} dt$ (or $\int_{C_L}^{\infty} \lambda e^{-\lambda t} dt) = e^{-\lambda C_S}$ (or $e^{-\lambda C_L}$), depending on the type of DRX cycle. Active and sleeping state time extensions are terminated with probabilities $e^{-\lambda C_T}$ and $1 - e^{-\lambda C_S}$ (or $1 - e^{-\lambda C_L}$), respectively. Consequently, the time duration increments for both states follow geometric distributions since these increments are determined by whether the packet arrives or not within inactivity timeout or short or long DRX cycle. Now, we represent the corresponding increment probabilities φ_i and ψ_j for active and sleeping states by

$$\varphi_i = (1 - e^{-\lambda C_T})^i e^{-\lambda C_T} \tag{2}$$

where $i \geq 0$. i indicates how many times the inactivity timer restarts until its expiration

$$\psi_j = \begin{cases} (e^{-\lambda C_S})^{j-1}(1-e^{-\lambda C_S}), & 1 \leq j \leq N \\ (e^{-\lambda C_S})^N (e^{-\lambda C_L})^{j-(N+1)}(1-e^{-\lambda C_L}), & N < j \end{cases} \tag{3}$$

where j indicates the number of short and long DRX cycles. Assuming that $E[t_S]$ and $E[t_L]$ are the average times where short and long DRX cycles last, respectively, we can have the time durations for both states by

$$\begin{aligned} E[T_A] &= E[\tilde{t}_B] + \sum_{i=0}^{\infty} i\varphi_i \left(E[\hat{t}_I] + E[t_B]\right) + C_T \\ &= E[\tilde{t}_B] + \left(E[\hat{t}_I] + E[t_B]\right)\left(e^{\lambda C_T} - 1\right) + C_T \end{aligned} \tag{4}$$

$$\begin{aligned} E[T_D] &= E[t_S] + E[t_L] \\ &= \sum_{j=1}^{N} j\psi_j C_S + \sum_{j=N+1}^{\infty} (j-N)\psi_j C_L \\ &= \frac{1-(e^{-\lambda C_S})^N}{1-e^{-\lambda C_S}} C_S + \frac{(e^{-\lambda C_S})^N}{1-e^{-\lambda C_L}} C_L. \end{aligned} \tag{5}$$

Accordingly, we need to derive $E[\hat{t}_I]$, $E[t_B]$, and $E[\tilde{t}_B]$. As discussed earlier, random variable $\hat{t}_I$ follows a truncated exponential distribution. Therefore, the probability density function (pdf) $f_{\hat{t}_I}(t)$ for the random variable $\hat{t}_I$ is given by

$$f_{\hat{t}_I}(t) = \begin{cases} \frac{1}{1-e^{-\lambda C_T}} \lambda e^{-\lambda t}, & 0 \leq t \leq C_T \\ 0, & C_T < t. \end{cases} \tag{6}$$

From this equation, we can derive $E[\hat{t}_I]$ by

$$\begin{aligned} E[\hat{t}_I] &= \int_0^{\infty} t f_{\hat{t}_I}(t)\, dt \\ &= \frac{1}{1-e^{-\lambda C_T}} \int_0^{C_T} \lambda t e^{-\lambda t}\, dt \\ &= \frac{1}{\lambda} - \frac{1}{e^{\lambda C_T} - 1} C_T. \end{aligned} \tag{7}$$

Random variable t_B begins with a new packet arrival and lasts as long as new packets arrive during buffered packet transmission times. In addition, we know that the number of packet arrivals can be modeled with the Poisson process since packet arrivals follow an exponential distribution. Then, we simply derive the average number packet arrivals during the transmission time for a single packet by $\sum_{n=0}^{\infty}((\lambda\tau)^n/n!)e^{-\lambda\tau} = \lambda\tau = \rho$. It implies that a single packet transmission generates additional ρ packets, and these packets need $\tau\rho$ transmission time for their transmissions. The generation recursively repeats infinitely. Finally, we can have $E[t_B]$ by

$$E[t_B] = \sum_{n=0}^{\infty} \tau\rho^n = \tau/(1-\rho). \tag{8}$$

The first activity period begins with the packets buffered during the DRX cycles prior to the first activity period. Therefore, $\lambda E[T_D]$ packets are buffered at the beginning of the first activity period. Therefore, we have the first activity period in the same manner as (8) by

$$E[\tilde{t}_B] = \lambda E[T_D] \frac{\tau}{1-\rho} = E[T_D] \frac{\rho}{1-\rho}. \tag{9}$$

From (7)–(9), we obtain $E[T_A]$ by

$$E[T_A] = \frac{\rho}{1-\rho} E[T_D] + \frac{1}{\lambda(1-\rho)}(e^{\lambda C_T} - 1). \tag{10}$$

Now, we summarize the power-saving factor shown in

$$\begin{aligned} &\frac{E[T_D]}{E[T_D] + E[T_A]} \\ &= \frac{E[T_D](1-\rho)}{E[T_D] + \frac{1}{\lambda}(e^{\lambda C_T} - 1)} \\ &= (1-\rho) \times \left(\frac{1-(e^{-\lambda C_S})^N}{1-e^{-\lambda C_S}} C_S + \frac{(e^{-\lambda C_S})^N}{1-e^{-\lambda C_L}} C_L \right) \\ &\quad \Big/ \left(\frac{1-(e^{-\lambda C_S})^N}{1-e^{-\lambda C_S}} C_S + \frac{(e^{-\lambda C_S})^N}{1-e^{-\lambda C_L}} C_L + \frac{1}{\lambda}(e^{\lambda C_T} - 1) \right). \end{aligned} \tag{11}$$

B. Transmission Delay

In immediate-transmitting state, a newly arrived packet is immediately transmitted if RNC's buffer becomes empty. However, when the buffer is not empty, the arrived packets may suffer delay due to the residual time, which is attributed to ongoing packet transmission and queued packets in RNC's buffer. The observations are a typical feature of the M/G/1 queuing system, so that we can easily derive the average packet transmission delay for the M/G/1 queuing system with the Pollaczek-Khinchine formula. Accordingly, the packet transmission delay $E[D_I]$ in immediate-transmitting state is derived by [23]

$$E[D_I] = \frac{\lambda E[X^2]}{2(1-\rho)}. \tag{12}$$

Meanwhile, in buffering-and-forwarding state, packets may experience additional delay since the packets that arrived during sleeping state are not transmitted. Accordingly, there are two types of delays. One is caused by the residual time. The other is additional delay by the packet buffering operation during sleeping state. We obtain the delay due to residual time in the

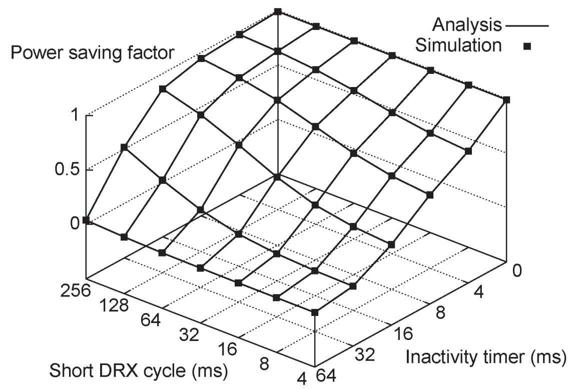

(a)

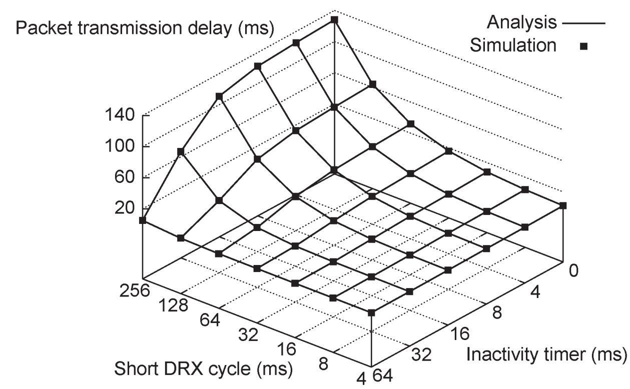

(b)

Fig. 3. Power-saving factor and average packet transmission delay when $N = 2$, $\tau = 0.1$, $\lambda = 0.1$, and $C_L = 2C_S$. (a) Power-saving factor. (b) Average packet transmission delay.

same way as (12), and hence, we need to derive the additional delay. For this purpose, we have two more notations, i.e., $E[K]$ and $E[W]$. $E[K]$ is the average number of waiting packets in RNC's transmission buffer in buffering-and-forwarding state. $E[W]$ is the average waiting time of the packets arrived from the last DRX cycle. Herein, we can represent the additional delay due to the buffering operation $E[D_B]$ by

$$E[D_B] = E[W] + E[X]E[K]. \tag{13}$$

According to Little's Law, $E[K] = \lambda E[D_B]$. From this equation, we can rearrange (13) by

$$\begin{aligned} E[D_B] &= E[W] + E[X]E[K] \\ &= E[W] + \lambda\tau E[D_B] \\ &= E[W] + \rho E[D_B] \\ &= \frac{E[W]}{1-\rho}. \end{aligned} \tag{14}$$

In buffering-and-forwarding state, one ore more packet arrivals during any DRX cycle initiate the first activity period at the end of the DRX cycle. Then, the DRX cycle becomes the last DRX cycle prior to the first activity period. It is needed to derive the average waiting time that the arrived packets in the last DRX cycle have to wait until the beginning of the first activity period. According to the property of the Poisson process, packet arrival time instants are uniformly distributed in the duration of the last DRX cycle [22]. Simply, we can obtain $E[W] = C_S/2$ or $C_L/2$, depending on which the packets arrive at, i.e., short or long DRX cycle.

In the steady state, $\lambda(E[T_A] + E[T_D])$ packets arrive during $E[T_A] + E[T_D]$, whereas $\lambda E[t_S]$ and $\lambda E[t_L]$ packets arrive during $E[t_S]$ and $E[t_L]$, respectively. Therefore, we can derive probabilities P_S and P_L that packets suffer delays of $C_S/2$ and $C_L/2$, respectively, by

$$\begin{aligned} P_S &= \frac{\lambda E[t_S]}{\lambda\left(E[T_A] + E[T_D]\right)} \\ P_L &= \frac{\lambda E[t_L]}{\lambda\left(E[T_A] + E[T_D]\right)}. \end{aligned} \tag{15}$$

From (12)–(15), we obtain the average packet transmission delay by

$$\begin{aligned} E[D] =& (1-P_S-P_L)E[D_I] \\ &+ P_S\left(E[D_I] + \frac{C_S}{2(1-\rho)}\right) + P_L\left(E[D_I] + \frac{C_L}{2(1-\rho)}\right) \\ =& \frac{\lambda E[X^2]}{2(1-\rho)} \\ &+ \frac{1}{2}\left(\frac{1-(e^{-\lambda C_S})^N}{1-e^{-\lambda C_S}}(C_S)^2 + \frac{(e^{-\lambda C_S})^N}{1-e^{-\lambda C_L}}(C_L)^2\right) \Bigg/ \\ &\left(\frac{1-(e^{-\lambda C_S})^N}{1-e^{-\lambda C_S}}C_S + \frac{(e^{-\lambda C_S})^N}{1-e^{-\lambda C_L}}C_L + \frac{1}{\lambda}(e^{\lambda C_T}-1)\right). \end{aligned} \tag{16}$$

IV. Evaluation

A. Results

We verify the analytical model by comparing analytical results with simulation results. We develop a simulator written in "C" language. It is working in Linux environments, and we have more than 100 000 runs for each averaged point of the figures. For simulation parameters, we have expected packet transmission time($= \tau$), average packet arrival rate($= \lambda$), and short DRX cycle($= C_S$) equal to 0.1 ms, 0.1/ms, and 8 ms, respectively.

As shown in Figs. 3 and 4, well-matched results show that numerical equations are correctly derived. In Fig. 3, we observe how both the power-saving factor and average packet transmission delay vary according to the DRX cycle, and the inactivity timer timeout conditioned that a long DRX cycle is twice the short DRX cycle. This figure shows that the power-saving factor and average packet transmission delay increase in proportion to the short DRX cycle when the inactivity timer has small values of timeout. However, when the inactivity timer has a long timeout, we can achieve good average packet transmission delay at the sacrifice of the power-saving factor.

In Fig. 4, we investigate the power-saving factor and average packet transmission delay, depending on the maximum number $(= N)$ of short DRX cycle for new packet arrival waiting, i.e., N *index* and the ratio between short and long DRX

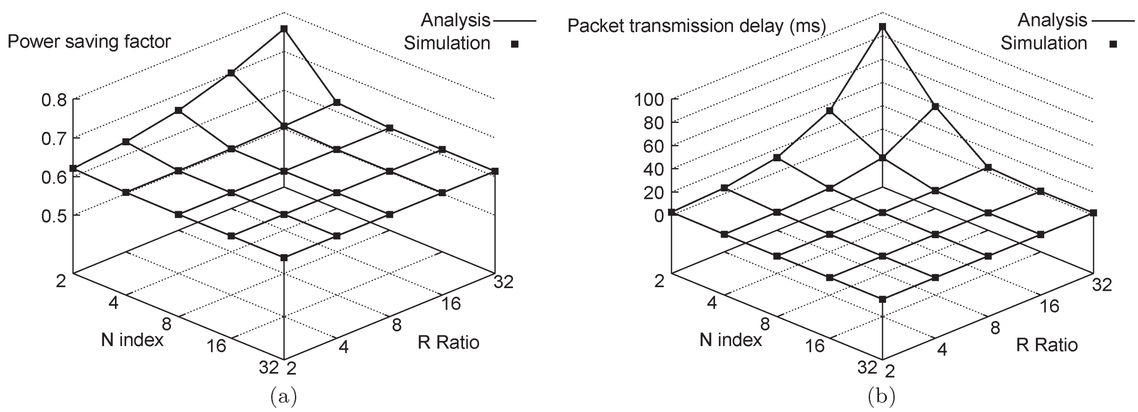

Fig. 4. Power-saving factor and average packet transmission delay when $\tau = 0.1$ ms, $\lambda = 0.1$/ms, $C_S = 8$ ms, and $C_T = 8$ ms. (a) Power-saving factor. (b) Average packet transmission delay.

cycles, i.e., R ratio$(=$ long DRX cycle/short DRX cycle$)$. The figure shows that the power-saving factor and average packet transmission delay change only when the R ratio is high and the N index is small. It implies that it is more likely that sleeping state UE utilizes a long DRX cycle after a small number of short DRX cycles. In this case, the UE suffers a long average packet transmission delay.

B. Further Consideration

So far, we have derived the power-saving factor and average packet transmission delay predicated on the proposed approach toward analytical studies, and we may apply the proposed approach for an extended power-saving operation. For example, we can imagine a system having two types of wireless interfaces for 3GPP LTE Advanced and ZigBee networks, respectively [10]. ZigBee is a wireless interface for low power consumption and low transmission rate. We can find similar applications in [17] and [31]. Simply, it is periodically activated to transmit packets buffered during sleeping time. Upon completion of the packet transmissions, it goes back to sleeping. We assume that the system alternatively utilizes those wireless interfaces, depending on packet arrival rates. In addition, both wireless interfaces are conducting power-saving operations.

First, we can divide the system into two independent parts for 3GPP LTE Advanced and ZigBee networks, respectively, depending on the condition determined by a packet arrival rate. We continue to segment two independent parts into several parts according to the state transition conditions in each network. In both 3GPP LTE Advanced and ZigBee networks, power-saving operations can be characterized with active and sleeping parts. Specifically, in the 3GPP LTE Advanced network, the time duration of an individual part increases, depending on packet transmission times, inactivity timers, and DRX cycles. Similarly, in the ZigBee network, the time durations are determined by packet transmission times. Sleeping time is the remaining part of a period.

In all cases, transmission times can be obtained from the number of packets buffered during sleeping time. Additionally, the time duration increments can be solved with typical probability mass functions of geometric distribution when a condition determines whether the time durations increase. In other words, all we need to do is to divide the power-saving operation into several independent parts according to state transition conditions. Then, we adapt the probability mass functions for each independent part of an extended power-saving operation or obtain the number of buffered packets for sleeping time.

Recall that the overall time duration for a power-saving operation is the sum of the time durations corresponding to the independent parts and the power-saving factor is a ratio between sleeping time duration and overall time duration. Similarly, the average packet transmission delay is derived with the time durations for the independent parts. Then, we can build aggregate equations reflecting the feature of an extended power-saving operation.

V. Conclusion

We provide an easy way to reach the accurate analytical model for the performance evaluation of the DRX operation in 3GPP LTE Advanced wireless networks. For this purpose, we develop a new approach by dividing the DRX operation into several independent parts and then combine the result obtained in each part. From the proposed analytical model, we obtain accurate power-saving factor and packet transmission delay without sophisticated mathematical techniques. Our approach will contribute to future work regarding the performance analysis of power-saving operations in various wireless networks since it can be easily extended and applied for further studies.

References

[1] Third-Generation Partnership Project, Tech. Spec. 3G TS 25.304 ver. 5.9.0, Sep. 2005.
[2] *Part 11: Wireless LAN Medium Access Control (MAC) and Physical Layer (PHY) Specifications, (Revision of IEEE Std 802.11-1999)*, IEEE Std. 802.11-2007, Jun. 2006.
[3] *Part 16: Air Interface for Broadband Wireless Access Systems*, IEEE Std. 802.16-2009, May 2009.
[4] Third-Generation Partnership Project, Tech. Spec. 3G TS 36.300 ver. 10.0.0, Jun. 2010.
[5] Third-Generation Partnership Project, Tech. Spec. 3G TS 36.304 ver. 10.0.0, Dec. 2010.
[6] *Part 16: Air Interface for Broadband Wireless Access Systems: Advanced Air Interface*, IEEE Std. 802.16m, May 2011.
[7] S. Baek, J. J. Son, and B. D. Choi, "Performance analysis of sleep mode operation for IEEE 802.16m advanced WMAN," in *Proc. IEEE ICC*, Jun. 2009, pp. 1–4.

[8] C. S. Bontu and E. Illidge, "DRX mechanism for power saving in LTE," *IEEE Commun. Mag.*, vol. 47, no. 6, pp. 48–55, Jun. 2009.
[9] K. De Turck, S. De Vuyst, D. Fiems, S. Wittevrongel, and H. Bruneel, "Performance of the sleep-mode mechanism of the new IEEE 802.16m proposal for correlated downlink traffic," in *Proc. NET-COOP*, Nov. 2009, pp. 152–165.
[10] S. Farahani, *ZigBee Wireless Networks and Transceivers*. Newton, MA: Newnes, 2008.
[11] E. Hwang, K. J. Kim, J. J. Son, and B. D. Choi, "The power saving mechanism with binary exponential traffic indications in the IEEE 802.16e/m," *Queueing Syst.*, vol. 62, no. 3, pp. 197–227, Jul. 2009.
[12] E. Hwang, K. J. Kim, J. J. Son, and B. D. Choi, "The power-saving mechanism with periodic traffic indications in the IEEE 802.16e/m," *IEEE Trans. Veh. Technol.*, vol. 59, no. 1, pp. 319–334, Jan. 2010.
[13] S. Jin, X. Chen, D. Qiao, and S. Choi, "Adaptive sleep mode management in IEEE 802.16m wireless metropolitan area networks," *Comput. Netw.*, vol. 55, no. 16, pp. 3774–3783, Nov. 2011.
[14] S. Jin, M. Choi, and S. Choi, "Performance analysis of IEEE 802.16m sleep mode for heterogeneous traffic," *IEEE Commun. Lett.*, vol. 14, no. 5, pp. 405–407, May 2010.
[15] S. Jin, K. Han, and S. Choi, "Idle mode for deep power save in IEEE 802.11 WLANs," *J. Commun. Netw.*, vol. 12, no. 5, pp. 480–491, Oct. 2010.
[16] S. Jin, C. Yoon, and S. Choi, "A simple remedy for idle mode via proxy MIP," *IEEE Commun. Lett.*, vol. 12, no. 6, pp. 423–425, Jun. 2008.
[17] T. Jin, G. Noubir, and B. Sheng, "WiZi-cloud: Application-transparent dual zigbee-WiFi radios for low power internet access," in *Proc. IEEE INFOCOM*, Apr. 2011, pp. 1593–1601.
[18] R. K. Kalle, M. Raj, and D. Das, "A novel architecture for IEEE 802.16m subscriber station for joint power saving class management," in *Proc. COMSNETS*, Jan. 2009, pp. 1–10.
[19] H. Levy and L. Kleinrock, "A queue with starter and a queue with vacations: Delay analysis by decomposition," *Oper. Res.*, vol. 34, no. 3, pp. 426–436, May/Jun. 1986.
[20] F.-W. Li, Y.-Q. Zhang, and L.-W. Li, "Enhanced discontinuous reception mechanism for power saving in TD-LTE," in *Proc. ICCSIT*, Sep. 2010, pp. 682–686.
[21] Y. Y. Mihov, K. M. Kassev, and B. P. Tsankov, "Analysis and performance evaluation of the DRX mechanism for power saving in LTE," in *Proc. IEEE IEEEI*, Nov. 2010, pp. 000520–000524.
[22] S. M. Ross, *Stochastic Processes*. New York: Wiley, 1983.
[23] H. Takagi, *Queueing Analysis: A Foundation of Performance Evaluation*. Amsterdam, The Netherlands: North–Holland, 1991.
[24] S.-R. Yang, "Dynamic power saving mechanism for 3G UMTS system," *Mobile Netw. Appl.*, vol. 12, no. 1, pp. 5–14, Jan. 2007.
[25] S.-R. Yang, P. Lin, and P.-T. Huang, "Modeling power saving for GAN and UMTS interworking," *IEEE Trans. Wireless Commun.*, vol. 7, no. 12, pp. 5326–5335, Dec. 2008.
[26] S.-R. Yang and Y.-B. Lin, "Modeling UMTS discontinuous reception mechanism," *IEEE Trans. Wireless Commun.*, vol. 4, no. 1, pp. 312–319, Jan. 2005.
[27] S.-R. Yang, S.-Y. Yan, and H.-N. Hung, "Modeling UMTS power saving with bursty packet data traffic," *IEEE Trans. Mobile Comput.*, vol. 6, no. 12, pp. 1398–1409, Dec. 2007.
[28] S. Yang, M. Yoo, and Y. Shin, "Adaptive discontinuous reception mechanism for power saving in UMTS," *IEEE Commun. Lett.*, vol. 11, no. 1, pp. 40–42, Jan. 2007.
[29] J.-H. Yeh, J.-C. Chen, and C.-C. Lee, "Comparative analysis of energy-saving techniques in 3GPP and 3GPP2 systems," *IEEE Trans. Veh. Technol.*, vol. 58, no. 1, pp. 432–448, Jan. 2009.
[30] L. Zhou, H. Xu, H. Tian, Y. Gao, L. Du, and L. Chen, "Performance analysis of power saving mechanism with adjustable DRX cycles in 3GPP LTE," in *Proc. VTC*, Oct. 2008, pp. 1–5.
[31] R. Zhou, Y. Xiong, G. Xing, L. Sun, and J. Ma, "ZiFi: Wireless LAN discovery via ZigBee interference signatures," in *Proc. ACM MobiCom*, Sep. 2010, pp. 49–60.

Sunggeun Jin (M'08) received the B.S. and M.S. degrees from Kyungpook National University, Daegu, Korea, in 1996 and 1998, respectively, and the Ph.D. degree from Seoul National University, Seoul, Korea, in August 2008.

In 1998, he joined ETRI, Daejeon, Korea, where he is currently an Engineer. He has participated in standard developments, including IEEE 802.11v, IEEE 802.16j, IEEE 802.16m, and IEEE 802.11ad. He is currently attending a new task group for Peer-Aware Communication in the 802.15 working group.

Dr. Jin has served as a Technical Program Committee member for the 2008 IEEE Wireless Communications and Networking Conference, the 2009 International Conference on Ubiquitous and Future Networks, the 2010 International Conference on Broadband Communications, Networks, and Systems, IEEE GLOBECOM 2011, and IEEE GLOBECOM 2012.

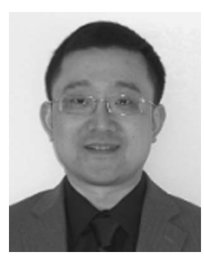

Daji Qiao (M'04) received the Ph.D. degree in Electrical Engineering: Systems, from the University of Michigan, Ann Arbor, in February 2004.

He is currently an Associate Professor with the Department of Electrical and Computer Engineering, Iowa State University, Ames. His current research interests include protocol and algorithm innovation and implementation for IEEE 802.11 wireless local area networks and wireless sensor networks, as well as pervasive computing applications.

Dr. Qiao is a member of the Association of Computing Machinery.